Journal of Nuclear Materials 398 (2010) 49–58

Contents lists available at ScienceDirect

Journal of Nuclear Materials

journal homepage: www.elsevier.com/locate/jnucmat

Proton irradiation effects on tensile and bend-fatigue properties of welded F82H specimens

S. Saito [a,*], K. Kikuchi [a], D. Hamaguchi [a], K. Usami [b], A. Ishikawa [b], Y. Nishino [b], S. Endo [b], M. Kawai [c], Y. Dai [d]

[a] JAEA Tokai, J-PARC Center, 2-4 Shirakata-shirane, Tokai-mura, Naka-gun, Ibaraki-ken 319-1195, Japan
[b] JAEA Tokai, Department of Hot Laboratories, Tokai-mura, Ibaraki-ken 319-1195, Japan
[c] KEK, Tsukuba-shi, Ibaraki-ken 305-0801, Japan
[d] PSI, Spallation Source Division, 5232 Villigen PSI, Switzerland

A B S T R A C T

In several institutes, research and development for an accelerator-driven transmutation system (ADS) have been progressed. Ferritic/martensitic (FM) steels are the candidate materials for the beam window of ADS. To evaluate of the mechanical properties of the irradiated materials, the post irradiation examination (PIE) work of the SINQ (Swiss spallation neutron source) target irradiation program (STIP) specimens was carried out at JAEA. In present study, the results of PIE on FM steel F82H and its welded joint have been reported. The present irradiation conditions of the specimens were as follows: proton energy was 580 MeV. Irradiation temperatures were ranged from 130 to 380 °C, and displacement damage level was ranged from 5.7 to 11.8 dpa. The results of tensile tests performed at 22 °C indicated that the irradiation hardening occurred with increasing the displacement damage up to 10.1 dpa at 320 °C irradiation. At higher dose (11.8 dpa) and higher temperature (380 °C), irradiation hardening was observed, but degradation of ductility was relaxed in F82H welded joint. In present study, all specimens kept its ductility after irradiation and fractured in ductile manner. The results on bend-fatigue tests showed that the fatigue life (N_f) of F82H base metal irradiated up to 6.3 dpa was almost the same with that of unirradiated specimens. The N_f of the specimens irradiated up to 9.1 dpa was smaller than that of unirradiated specimens. Though the number of specimen was limited, the N_f of F82H EB (15 mm) and EB (3.3 mm) welded joints seemed to increase after irradiation and the fracture surfaces of the specimens showed transgranular morphology. While F82H TIG welded specimens were not fractured by 10^7 cycles.

1. Introduction

In several institutes, research and development for an accelerator-driven transmutation system (ADS) to transmute minor actinide (MA) have been progressed. ADS is composed of high-energy proton accelerator, lead–bismuth eutectic (LBE) spallation target and sub-critical core including MA fuel. Accelerated protons injected to spallation target through target beam window produce high-energy neutrons by spallation reaction. The spallation reaction region acts as an external neutron source for the MA fuel sub-critical core. Therefore, the target beam window and the structural materials in the reactor will be subjected to high-energy proton and spallation neutron irradiation.

Ferritic/martensitic (FM) steels are considered as the material for the target beam window materials of ADS. Because FM steels, as comparing to austenitic stainless steels, have higher strength, better thermal mechanical properties, better irradiation properties under fission neutron [1] and superior corrosion resistance to LBE. Among the various types of FM steels, the (7–9)Cr–(1–2)W FM steels, for instance F82H, are considered as tentative materials for nuclear applications because of their smaller DBTT shifts and their lower induced activation after irradiation [2]. F82H has been developed for fusion reactor blanket material and database including fission neutron irradiation have been established [3]. On the other hand, proton or spallation irradiation data are very limited. To obtain the proton irradiation data, materials irradiation programs were done at PSI and LANSCE. Until now, data on the tensile properties of the proton-irradiated F82H were reported [4–7]. However there are no data on bend-fatigue properties of F82H irradiated in spallation environment. The purpose of this study is to investigate irradiation effects on the mechanical properties of F82H. For the purpose, the post irradiation examination (PIE) work on STIP (SINQ target irradiation program) [8,9] specimens was car-

* Corresponding author. Tel.: +81 29 282 5058; fax: +81 29 282 6489.
E-mail address: saito.shigeru@jaea.go.jp (S. Saito).

0022-3115/$ - see front matter © 2009 Elsevier B.V. All rights reserved.
doi:10.1016/j.jnucmat.2009.10.009

Table 1
Chemical composition of F82H and TIG wire (wt.%).

wt.%	Fe	Cr	Ni	Mo	Mn	Ti	V	W	Ta	Cu	C	Si	P	S	N
F82H	Bal.	7.87	0.02	0.003	0.1	0.004	0.19	1.98	0.03	0.01	0.09	0.07	0.003	0.001	0.007
TIG wire	Bal.	7.7	–	–	–	–	0.2	2.0	0.02	–	0.08	–	–	–	–

ried out at JAEA for F82H and its welded joint. In this paper, the results of tensile tests and bend-fatigue tests on STIP specimens will be reported.

2. Experimental

2.1. Materials and specimens

The chemical composition of the F82H plates used in this study is given in Table 1. The hot rolled plates with a thickness of 15 mm were normalized at 1040 °C for about 38 min, followed by tempering at 750 °C for 1 h. The small tensile and bend-fatigue specimens used in this study are shown in Fig. 1. Size effect on tensile specimens of ferritic steel (JFMS, 10Cr–2Mo) was investigated by Kohyama et al. [10]. According to the paper, the specimen size of the present study does not affect the results of the tensile tests. Size effect on bend fatigue specimen of ferritic steel was not investigated. Specimens were cut from plates by EDM (Electrical Discharge Machining) and mechanically polished. The bend-fatigue specimens were taken from the plates.

TIG (tungsten inert gas) welded joints for the plates with a thickness of 15 mm were performed by using oscillating arc method with the electrode swinging. The electric current and voltage for the welded joint were 270–300 A (pulse) and 9–10 V, respectively. The welding speed was performed at a rate of 80 mm/min. The post-welding heat treatment (PWHT) was done at 720 °C for 1 h. The chemical composition of filler wire is shown in Table 1. Both the tensile and the bend-fatigue specimens were machined from the fusion zone vertical to weld line. Vicker's micro-hardness tests were performed for the specimens with a load of 50 gf and a holding time of 15 s. Fig. 2 shows the hardness profile of the TIG specimens. The hardness of the specimens decreased as compared with that of the base metal.

EB (electron beam) welded joints were produced by 15 mm and 3.3 mm thickness plates. For 15 mm EB welded joints, welding was conducted for plates the 15 mm thick without filler metal. EB welding were performed with an electron beam conditions of 200 mA and 90 kV. The welding speed was 400 mm/min. PWHT was not done. The tensile specimens were machined from the fusion zone parallel to weld line. Fig. 3 shows the hardness profile of the tensile specimen machined from the fusion zone. The hardness of the specimens increased as compared with that of the base metal. Meanwhile the bend-fatigue specimens were machined vertical to weld line. Necking part of the bend-fatigue specimens includes fusion zone and heat affected zone (HAZ). Hardness profile was not uniform at the necking part but showed double peaks distribution, because there was softening area at the center of the fusion zone. For 3.3 mm EB welded joints, the welding was conducted for the plates with 3.3 mm thickness without filler metal. EB welding were performed with an electron beam conditions of 9 mA and 150 kV. The welding speed was performed under a

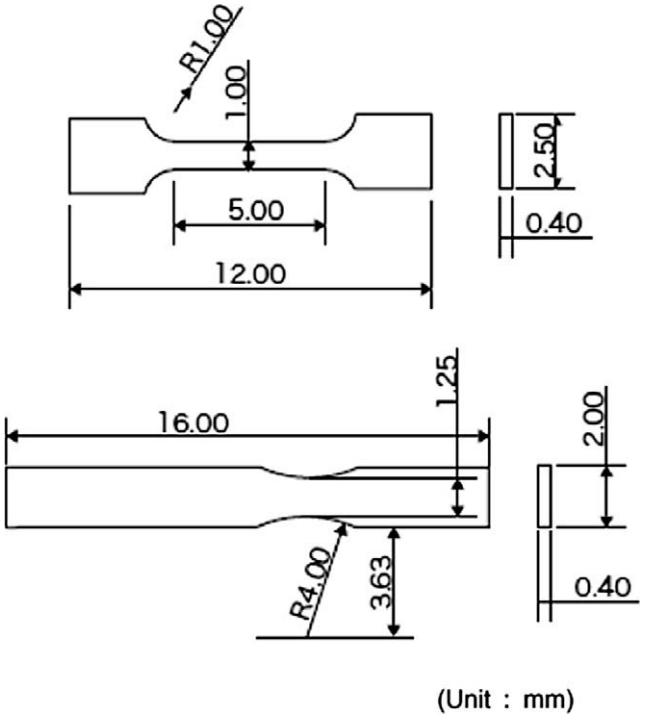

Fig. 1. Test specimens for tensile test (upper) and for bend-fatigue test (lower).

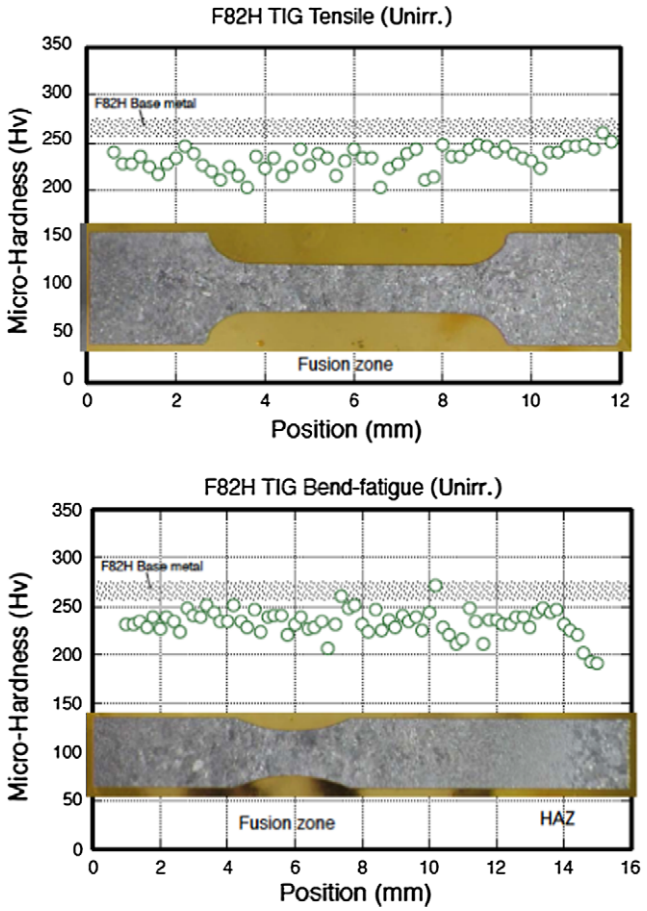

Fig. 2. The hardness profile of the unirradiated TIG specimens.

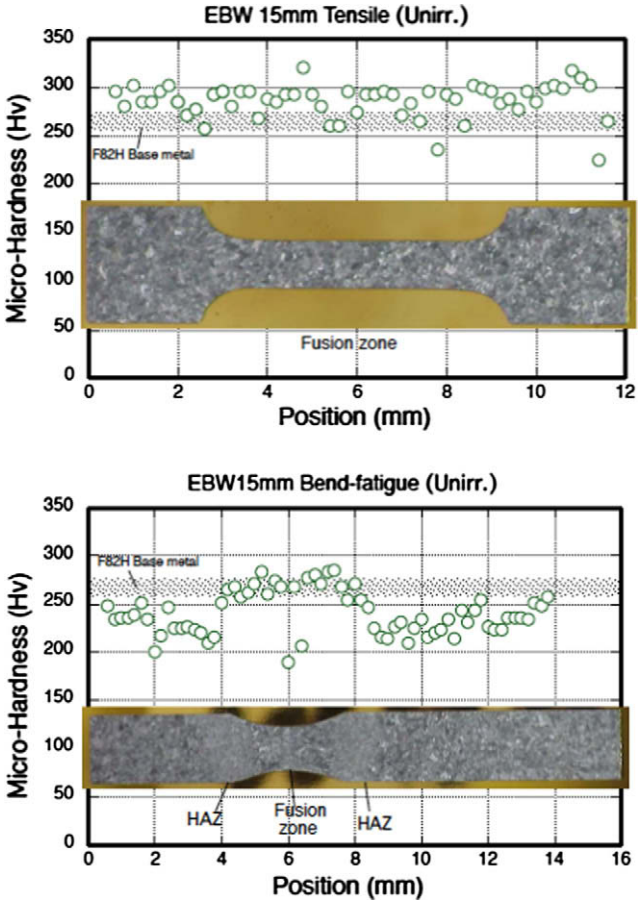

Fig. 3. The hardness profile of the unirradiated EB (15 mm) specimens.

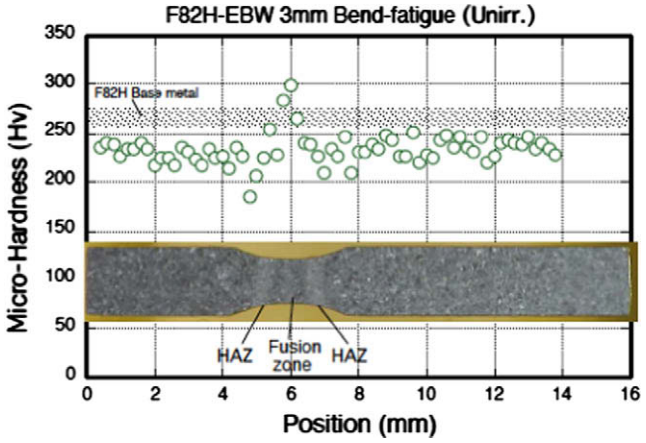

Fig. 4. The hardness profile of the unirradiated EB (3.3 mm) specimen.

condition of 600 mm/min. PWHT was done at 720 °C for 1 h. Fig. 4 shows the hardness profile of the EB (3.3 mm) specimen. Hardness profile was not uniform at the necking part but it had a peak value of 300 Hv in micro-hardness.

2.2. Irradiation

The 580 MeV proton irradiation was performed at SINQ-target 3 at the PSI. The irradiation temperatures were ranged from 135 °C to 380 °C. The damage levels were ranged from 5.7 to 11.8 dpa. Calculated helium and hydrogen production rates in steels are about 80 appm/dpa and 500 appm/dpa, respectively. Details of the irradiation have been reported by Dai and co-workers [8,9]. Irradiation conditions of JAEA specimens are summarized in Tables 2–4.

2.3. Post irradiation examinations

Tensile testing was performed in a screw driven type tensile machine. The machine was developed for the remote handling test in the hot cell. Specimens were strained at an initial rate of 6×10^{-4}/s (0.2 mm/min) from the both sides in order to keep a gauge part of the specimen almost at the same place in space during the loading. Strains were measured by image analyses. CCD camera and computer system were used for memorizing absolute coordinates of specimen marked as the boundary of colored area in the rectangular window and updating new window. Strains were calculated by the displacement of window between two points on the gauge part of the specimens [11]. Tensile tests were carried out at about 22 °C and 250 °C in air. A focused infrared ray heated specimens. Temperature control was done by the thermocouple.

The STIP specimens were very small so that we developed a new fatigue-testing machine with ceramic piezoelectric actuators [12]. All bend-fatigue tests were done at RT in air. The frequency was 26 Hz and its waveform was reversed sine curve.

The fracture surfaces of the tested specimens were observed by SEM of SHIMADZU EPM-810Q, and it was operated at 20 kV.

3. Results

3.1. Tensile tests on F82H welds

Tensile properties of unirradiated and irradiated F82H welds are summarized in Tables 2 and 3. The stress–strain curves of F82H welds tested at RT and 250 °C are shown in Figs. 5 and 6, respec-

Table 2
Irradiation conditions and tensile properties of the unirradiated and the irradiated F82H TIG specimens.

ID	Irradiation temperature (°C)	dpa	He (appm)[a]	H (appm)[a]	Test temperature (°C)	YS (MPa)	UTS (MPa)	UE (%)	TE (%)	RA (%)	True strain to plastic instability
Q05	–	0	–	–	21	541	654	5.7	16.0	85.2	0.082
Q06	–	0	–	–	23	552	656	5.4	15.1	81.8	0.096
Q14	–	0	–	–	21	576	696	5.6	14.8	83.8	0.100
Q03	140–166	5.7	456	2907	20	793	799	0.3	8.8	84.3	0.008
Q01	212–252	7.9	632	4029	19	848	848	0.2	7.8	73.3	0.008
Q08	261–310	10.1	808	5151	20	936	941	0.4	7.2	67.2	0.010
Q11	–	0	–	–	250	495	546	2.2	10.9	86.2	0.035
Q15	–	0	–	–	250	511	579	2.8	10.7	86.1	0.050
Q10	147–175	5.7	456	2907	250	620	625	0.4	7.3	79.1	0.006
Q02	201–239	7.9	632	4029	250	689	691	0.5	6.3	50.5	0.021
Q12	275–326	10.1	808	5151	250	–	–	–	–	68.8	–
Q07	321–381	11.8	944	6018	250	700	732	3.8	9.6	–	0.060

[a] Calculated value.

Table 3
Irradiation conditions and tensile properties of the unirradiated and the irradiated F82H EB specimens.

ID	Irradiation temperature (°C)	dpa	He (appm)[a]	H (appm)[a]	Test temperature (°C)	YS (MPa)	UTS (MPa)	UE (%)	TE (%)	RA (%)	True strain to plastic instability
R1	–	0	–	–	21	735	811	2.6	10.1	76.0	0.040
R2	–	0	–	–	22	739	901	3.0	12.7	73.0	0.052
R9	–	0	–	–	22	738	809	3.0	12.4	74.4	0.052
R10	137–163	5.7	456	2907	22	876	884	0.4	6.3	73.5	0.005
R07	198–235	7.9	632	4029	21	958	965	0.4	7.6	45.8	0.024
R05	256–305	10.1	808	5151	21	999	1011	0.4	5.2	62.5	0.014
R12	296–347	11.2	896	5712	22	900	912	1.6	6.1	–	0.052
R14	–	0	–	–	250	680	701	1.2	9.9	81.5	0.028
R15	–	0	–	–	250	721	751	1.3	10.1	82.2	0.021
R11	143–170	5.7	456	2907	250	719	819	0.1	6.0	75.8	0.010
R08	206–245	7.9	632	4029	250	799	803	0.3	4.6	42.8	0.006
R06	268–318	10.1	808	5151	250	876	892	0.5	4.0	40.6	0.020
R03	300–356	11.8	944	6018	250	868	880	0.6	3.9	–	–

[a] Calculated value.

Table 4
Irradiation conditions of the bend-fatigue specimens.

Material	ID	Irradiation temperature (°C)	dpa	He (appm)[a]	H (appm)[a]
F82H base metal	P43	140–134	6.3	504	3213
	P44	136–160	6.3	504	3213
	P45	204–239	9.1	728	4641
	P46	210–245	9.1	728	4641
F82H TIG	Q23	202–237	9.1	728	4641
	Q25	204–239	9.1	728	4641
	Q27	135–158	6.3	504	3213
	Q28	136–160	6.3	504	3213
F82H EB (15 mm)	R23	202–237	9.1	728	4641
	R25	135–158	6.3	504	3213
	R26	204–237	9.1	728	4641
	R27	136–160	6.3	504	3213
F82H EB (3.3 mm)	S32	140–134	6.3	504	3213
	S35	204–237	9.1	728	4641
	S37	210–245	9.1	728	4641
	S38	136–160	6.3	504	3213

[a] Calculated value.

tively. In these plots strains were calculated by engineering definition. The results indicate that several dpa irradiations caused considerable irradiation hardening and reduction of ductility.

3.1.1. 22 °C testing

The selected stress–strain curves of F82H TIG and EB tested at RT are shown in Fig. 5a and b, respectively. For the TIG specimens, Yield strength (YS) increased with increasing displacement damage up to 10.1 dpa below 310 °C irradiation. Uniform elongation (UE) and true strain to plastic instability defined by Considere's criterion [13] reduced by the irradiation. After the irradiation of 5.7–10.1 dpa, UE and the true strain to plastic instability fell into 0.2–0.4% and 0.008–0.01, respectively. Total elongation (TE) and reduction of area (RA) decreased with increasing displacement damage up to 10.1 dpa. TE decreased about a half value of the unirradiated specimens, 8.8–7.2%. RA of 5.7 dpa irradiated specimen was almost the same with that of the unirradiated specimens. After 7.9–10.1 dpa irradiation, RA fell into 73.3–67.2%.

In case of F82H EB specimens, YS increased with increasing dpa up to 10.1 dpa below 305 °C irradiation. Though at higher dose (11.2 dpa) and higher temperature (350 °C), irradiation hardening was decreased. UE and the true strain to plastic instability was reduced by the irradiation. After 5.7–10.1 dpa irradiation, UE and the true strain to plastic instability fell into 0.4% and 0.005–0.024, respectively. At 11.2 dpa irradiation, UE and the true strain to plastic instability increased to 1.6% and 0.052, respectively. Total elongation (TE) and reduction of area (RA) was decreased by the irradiation. There was no dose dependence of reduction of TE

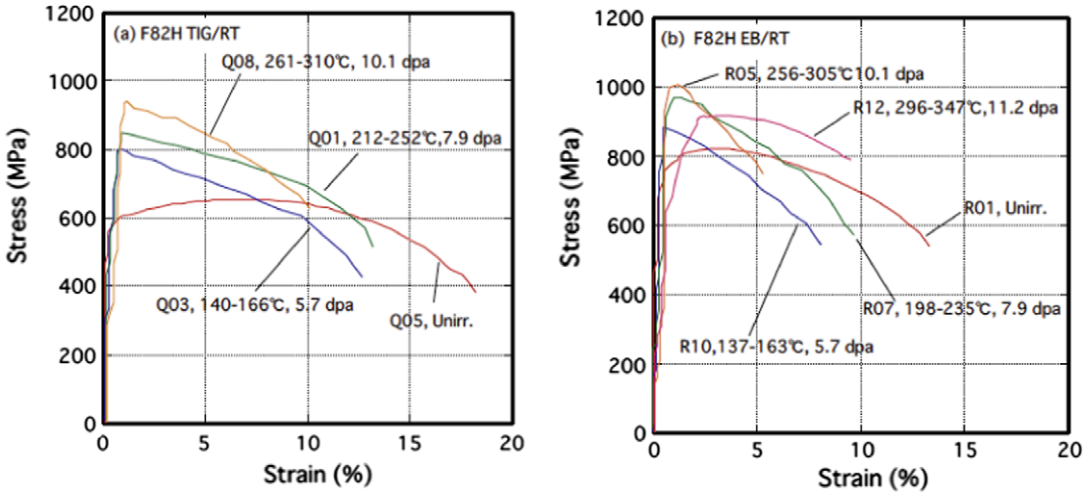

Fig. 5. Stress–strain curves of the unirradiated and the irradiated (a) F82H TIG and (b) F82H EB specimens tested at RT.

and RA. TE decreased about half value of the unirradiated specimens, 5.2–7.6%. RA of 5.7 dpa irradiated specimen was almost same with that of the unirradiated specimens. After 7.9 dpa irradiation, RA fell into minimum value of 45.8%. At 10.1 dpa irradiation, RA increased to 62.5%.

3.1.2. 250 °C testing

The selected stress–strain curves of F82H TIG and EB tested at 250 °C are shown in Fig. 6a and b, respectively. For TIG specimens, YS increased with increasing the displacement damage up to 11.8 dpa at below 380 °C irradiation. UE and true strain to plastic

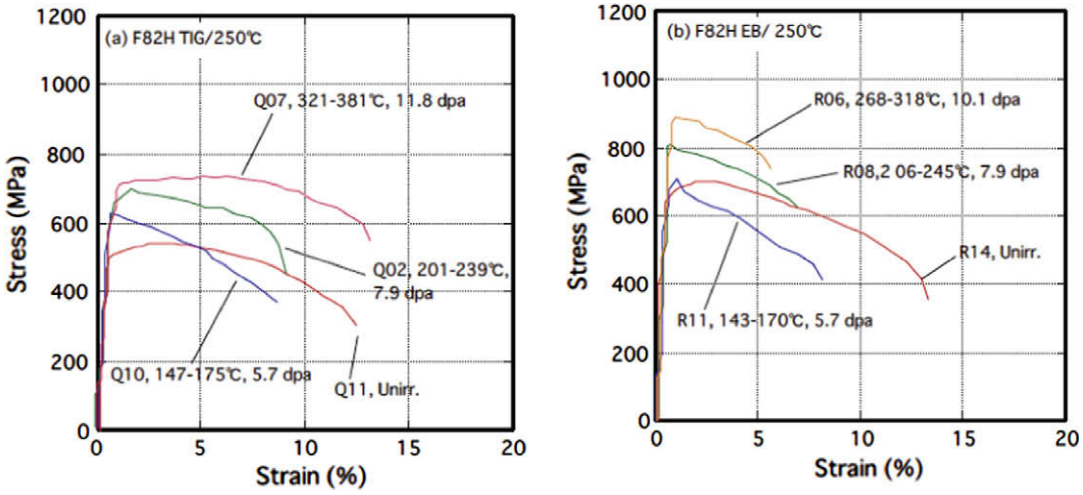

Fig. 6. Stress–strain curves of the unirradiated and the irradiated (a) F82H TIG and (b) F82H EB specimens tested at 250 °C.

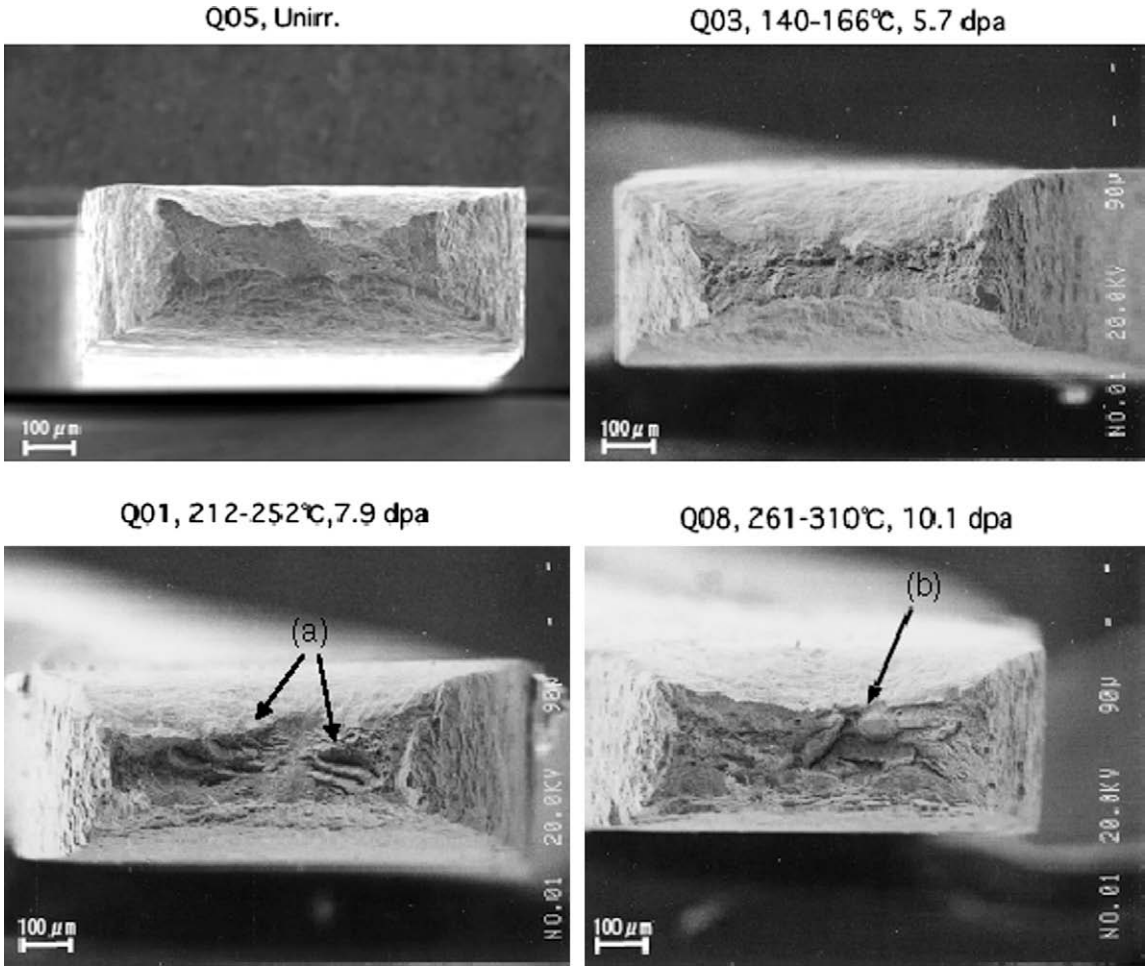

Fig. 7. SEM photographs of fracture surface of the unirradiated and the irradiated F82H TIG specimens tested at RT. The black arrows indicate (a) fringe like morphology and (b) unique morphology.

instability were reduced by the irradiation. After the irradiation of 5.7–7.9 dpa, UE and the true strain to plastic instability fell into 0.4–0.5% and 0.006–0.021, respectively. At 11.8 dpa irradiation, UE and the true strain to plastic instability increased to 3.8% and 0.06, respectively. TE was down to 6.3% by 7.9 dpa irradiation and was changed to 9.6% by 11.8 dpa irradiation at 380 °C. RA of 5.7 dpa irradiated specimen decreased to 79.1%. After 7.9 dpa irradiation, RA fell into minimum value of 50.5%. At 10.1 dpa irradiation, RA increased to 68.8%.

In case of F82H EB specimens, YS increased with increasing displacement damage up to 10.1 dpa at below 320 °C irradiation. Though the irradiation of higher dose of 11.8 dpa and higher temperature of 358 °C, irradiation hardening was reduced. UE and the true strain to plastic instability were decreased by the irradiation. After the irradiation of 5.7–10.1 dpa, UE and the true strain to plastic instability fell into 0.1–0.5% and 0.006–0.02, respectively. At 11.2 dpa, UE slightly increased to 0.6%. TE decreased with increasing displacement damage up to 10.1 dpa and fell into 6.0–3.9%. RA decreased with increasing displacement damage up to 10.1 dpa and fell into 75.8–40.6%.

3.1.3. Fracture surfaces

Figs. 7 and 8 show the SEM photographs of fracture surfaces of F82H TIG and F82H EB, respectively. The morphology of the fracture surface of both welds was changed with increasing displacement damage. Typical dimple patterns were observed in unirradiated specimens. Elongated dimples were observed in the irradiated specimens with 5.7 dpa. The morphology of the specimens was almost chisel edge fracture. For the irradiated specimens with 7.9 dpa, fringe like morphology (black arrow(a))were observed. For the irradiated TIG specimen with 10.1 dpa, unique morphology (black arrow(b)) was observed. For the irradiated EB specimen with 10.1 dpa, the deep valley was observed. In any case, specimens were fractured in a ductile manner.

3.2. Bend-fatigue tests

3.2.1. 22 °C testing

Bend-fatigue properties of unirradiated and irradiated F82H base metal and its welds tested at 22 °C are summarized in Table 4. Fig. 9a–d shows the relationship between total strain range and number of cycles to failure (N_f) on a log–log scale.

Fig. 9a shows the fatigue life of F82H BM. The fatigue life of the specimens with 6.3 dpa was almost the same with that of the unirradiated specimens. It seems that the fatigue life of the specimens irradiated up to 9.1 dpa was slightly reduced as compared with that of unirradiated specimens. Fig. 9b shows the fatigue life of F82H TIG specimens. The two specimens were tested at a maximum displacement, but it did not fracture up to 10^7 cycles. The remaining two specimens were not tested. Fig. 9c shows the fatigue life of F82H EB (15 mm) specimens. The one specimen fractured and the other two specimens did not fracture during 10^7 cycles. The remaining one specimen was not tested. Though the number of data is limited, the fatigue life of F82H EB (15 mm) seems to increase after the irradiation. Fig. 9d shows the fatigue life of F82H EB (3.3 mm) specimens. The two specimens fractured

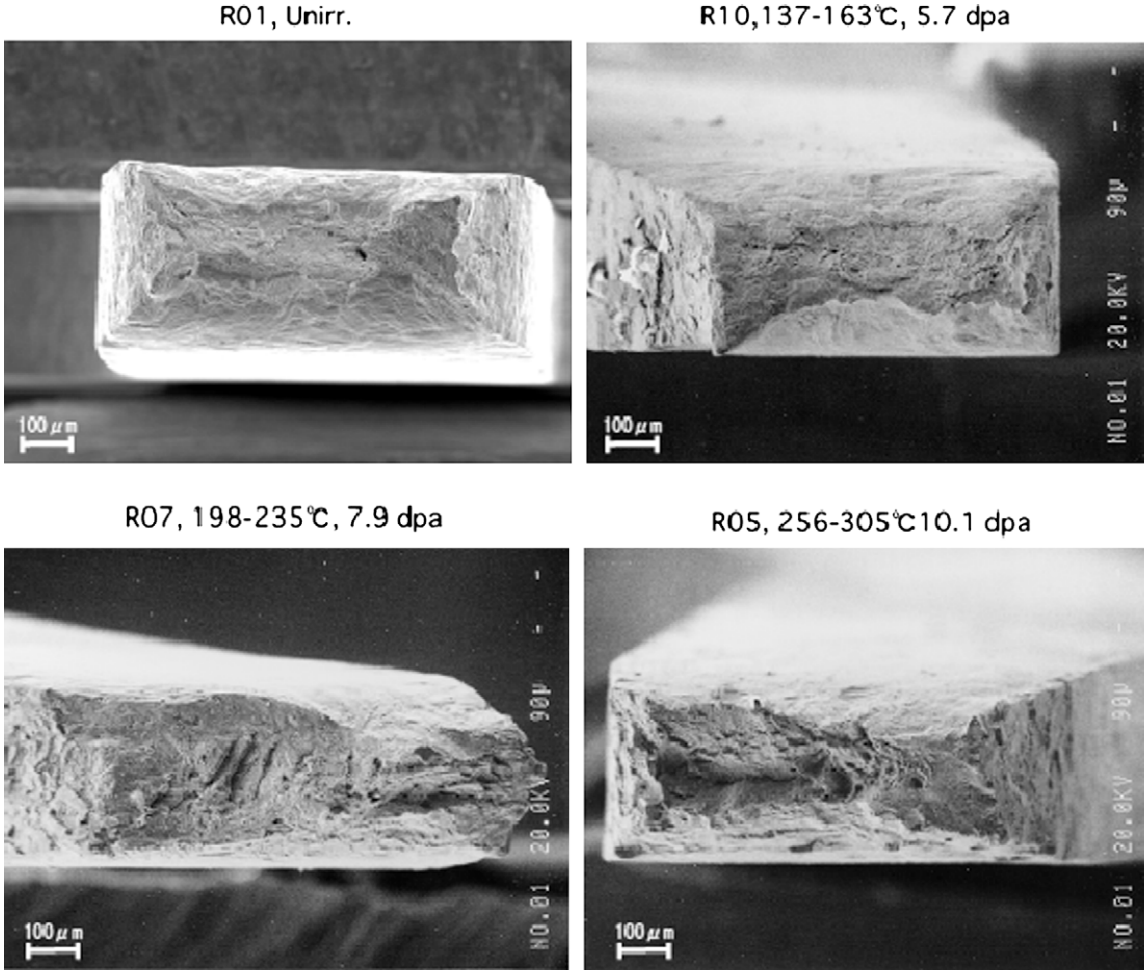

Fig. 8. SEM photographs of fracture surface of the unirradiated and the irradiated F82H EB specimens tested at RT.

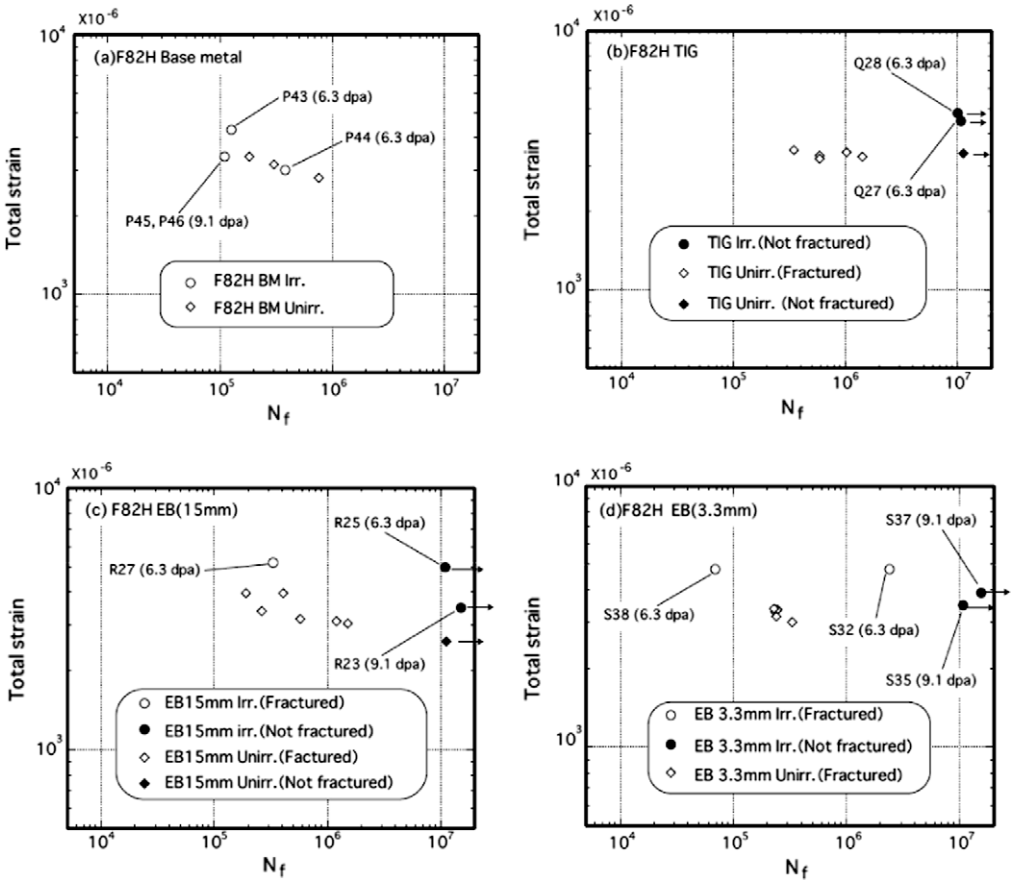

Fig. 9. The fatigue life of the unirradiated and the irradiated (a) F82H base metal, (b) F82H TIG, (c) F82H EB (15 mm) and (d) F82H EB (3.3 mm) specimens as the total strain range versus the number of cycles to failure (N_f) on a log–log scale.

and the other two specimens did not fracture during 10^7 cycles. Though the number of data is limited, the fatigue life of F82H EB (3.3 mm) tends to increase after the irradiation (see Table 5).

3.2.2. Fracture surfaces

Figs. 10 and 11 show the SEM photographs of fracture surfaces of F82H BM and EB (3.3 mm), respectively. For F82H BM specimens, the most part of fracture surfaces were observed as a transgranular morphology. However, 5–6% of intergranular fracture surface (black arrows in Fig. 10) was observed for both the unirradiated and irradiated specimens. The flatness of the surface was reduced by the irradiation. The EB (3.3 mm) specimens showed similar transgranular fracture surfaces. The flatness of the surface was reduced by the irradiation, which was similar to the base metal.

4. Discussion

4.1. Tensile properties

The comparison of the tensile properties on the proton-irradiated F82H welds and F82H BM are plotted in Fig. 12a and b. The data on F82H BM were taken from PSI experiment [5] and LANSCE experiment [7]. The irradiation temperature of PSI experiment and LANSCE experiment were 93–370 °C and <60 °C, respectively. Fig. 12a shows the relationship between the irradiation dose and increment of YS. All of the data was tested at R.T. The increment of YS of BM increased by 2–3 dpa irradiation. Above 3 dpa, the increment of YS increased and reached to over 500 MPa. Meanwhile the increase in YS of TIG and EB reached to about 370 MPa and 260 MPa, respectively. It was shown that the increase in YS or hardening of the proton-irradiated welds is less than that of BM. Fig. 12b shows the relationship between dpa and total elongation (TE). All of the data was obtained at R.T. The results show that TE in BM of LANSCE experiment reduced by 1–2 dpa irradiation. The reason of the reduction is thought to be attributed to low temperature (<60 °C) irradiation and large helium production rate in 800 MeV proton irradiation. TE in BM for PSI experiment and welds was reduced gradually up to 5.8 dpa irradiation, however, BM in PSI experiment lost its ductility by 9.8 dpa irradiation. The fracture surface of the specimen showed brittle intergranular morphology. The reason of the loss of ductility is still unknown [5]. While F82H welds specimens still have ductility up to 11 dpa irradiation.

4.2. Bend-fatigue properties

There are not many data on fatigue life of irradiated FM steels [14–20], and they are obtained by axial strain-controlled fatigue tests. There are no data on bend fatigue life of irradiated specimens. We will discuss the irradiation effects on fatigue life in these limited data. Some authors [14–18] reported that the fatigue life was reduced by irradiation. On the other hand, Grossbeck et. al. [19] concluded that little or no effect of irradiation was on the fatigue life. Furthermore, Bertsch et al. [20] showed that the fatigue life of irradiated specimen was reduced at high strain range ($\varepsilon_t = 0.9 \times 10^4$) test and was slightly increased at low strain range ($\varepsilon_t < 0.5 \times 10^4$) test. From these results, it is concluded that the irradiation effects on fatigue life of FM steels could be strongly affected by irradiation temperatures, test temperatures, strain

Table 5
Irradiation and test conditions of the fatigue tests on F/M steels.

Material	Irradiation temperature (°C)	dpa	He (appm)[a]	Irradiation	Strain range (10^{-6})	Fatigue life change	Reference
F82H	135–245	6.3–9.1	504–728	590 MeV proton and spallation neutron	$0.3–0.43 \times 10^4$	No change (6.3 dpa) Decreased (9.1 dpa)	Present study
F82H EB	135–245	6.3–9.1	504–728	590 MeV proton and spallation neutron	$0.3–0.52 \times 10^4$	Increased	Present study
F82H	90	0.02	–	Fission neutron (JMTR)	$1.0–2.0 \times 10^4$	Decreased	[13]
F82H	90	0.02	2.0×10^{-4}	Fission neutron (JMTR)	$0.6–2.0 \times 10^4$	Decreased	[14]
F82H	120	0.03	120	50 MeV alpha	$0.6–1.0 \times 10^4$	Decreased	[14]
F82H	250	3.8	–	Fission neutron (JRR-3)	$0.4–1.0 \times 10^4$	Decreased	[15]
DIN1.4914 (MANET, 12Cr)	90–430	0.01–0.7	1.3–91	590 MeV proton	$0.54–0.89 \times 10^4$	Decreased	[16]
DIN1.4914 (MANET, 12Cr)	420	1.6	400	104 MeV alpha	$0.5–1.0 \times 10^4$	Decreased	[17]
9Cr-1MoVNb	55	2.5–3.3	2–4	Fission neutron (HFIR)	$0.3–1.0 \times 10^4$	No change	[18]
12Cr–1MoVW (+Ni)	55	10–25	34–410	Fission neutron (HFIR)	$0.5–1.0 \times 10^4$	No change (No Ni doped) Decreased (1–2%Ni doped)	[18]
F82H	250	0.4–0.67	400	104 MeV alpha	$0.4–0.9 \times 10^4$	Decreased ($\varepsilon_t = 0.9 \times 10^4$) Increased ($\varepsilon_t < 0.5 \times 10^4$)	[19]

[a] Calculated value.

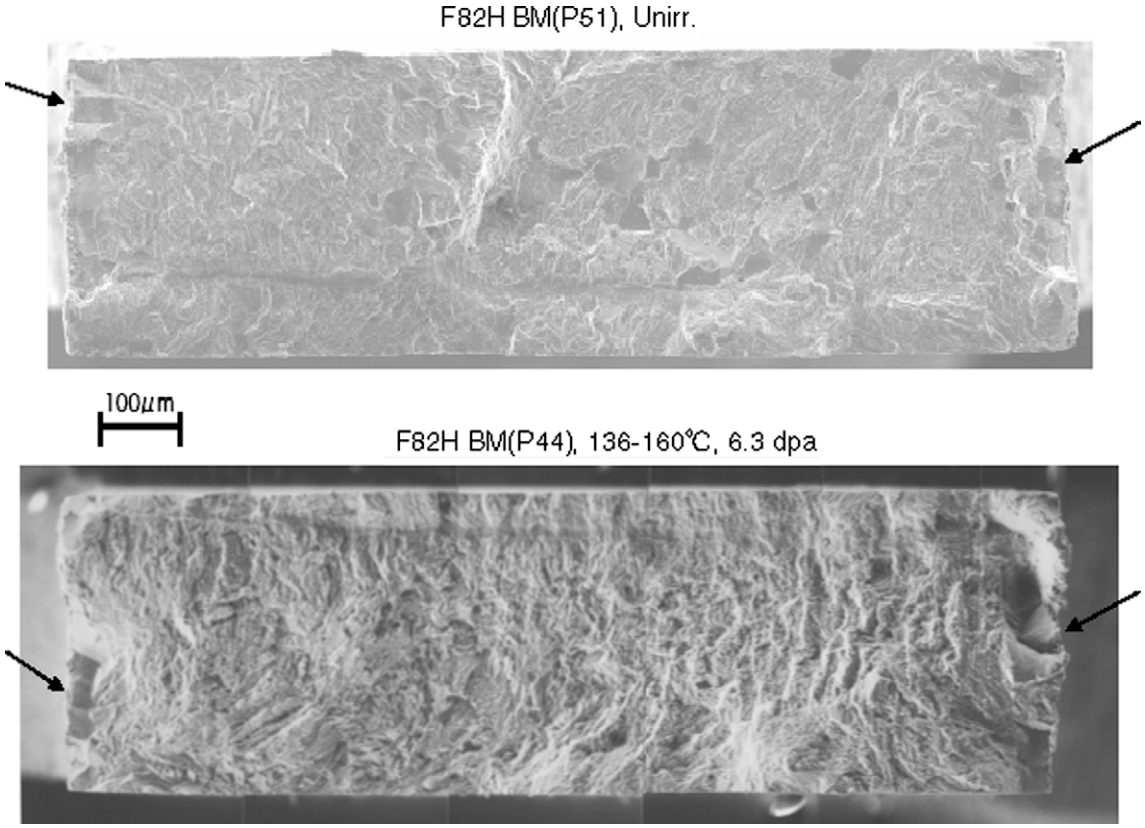

Fig. 10. Fracture surfaces of the unirradiated and the irradiated F82H base metal specimens. The black arrows indicate intergranular fracture surface.

ranges and He contents. In the experimental conditions, however, little change of the fatigue life was observed for the specimens irradiated to 6.3 dpa at 130–160 °C. Namely helium concentrations do not affect the fatigue properties, because helium atoms are not able to move easily at the low temperature. However, the results of the specimen irradiated to 9.1 dpa at 200–250 °C indicate a reduction of the fatigue life at higher temperature and higher dose irradiation. Further investigation will be necessary for fracture surface and microstructure.

There were no data in previous studies for the fatigue properties of the irradiated welds of reduced-activation FM steels. The results of present study indicate that the fatigue life of the irradiated welds increased in comparison with those from the unirradiated specimens. To explain the fact, metallographical observation, hardness profile measurement for the irradiated and the non-fractured specimens and microstructure investigation of the tested specimens will be required in future examinations.

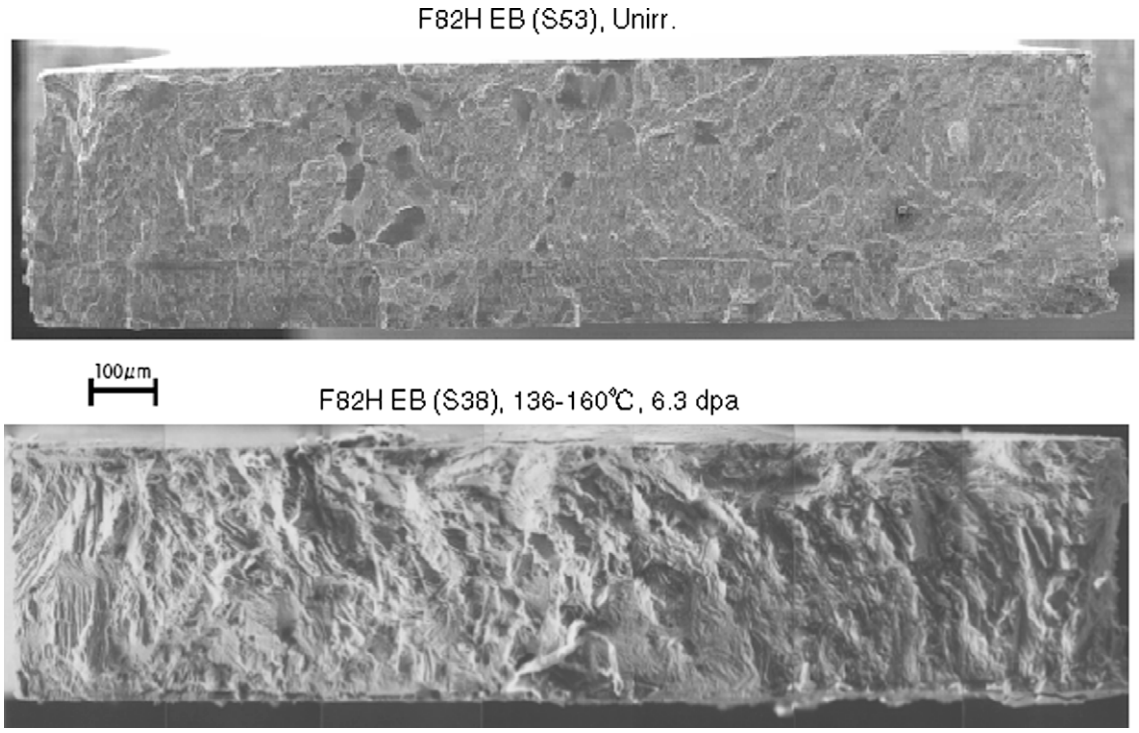

Fig. 11. Fracture surfaces of the unirradiated and the irradiated F82H EB (3.3 mm) specimens.

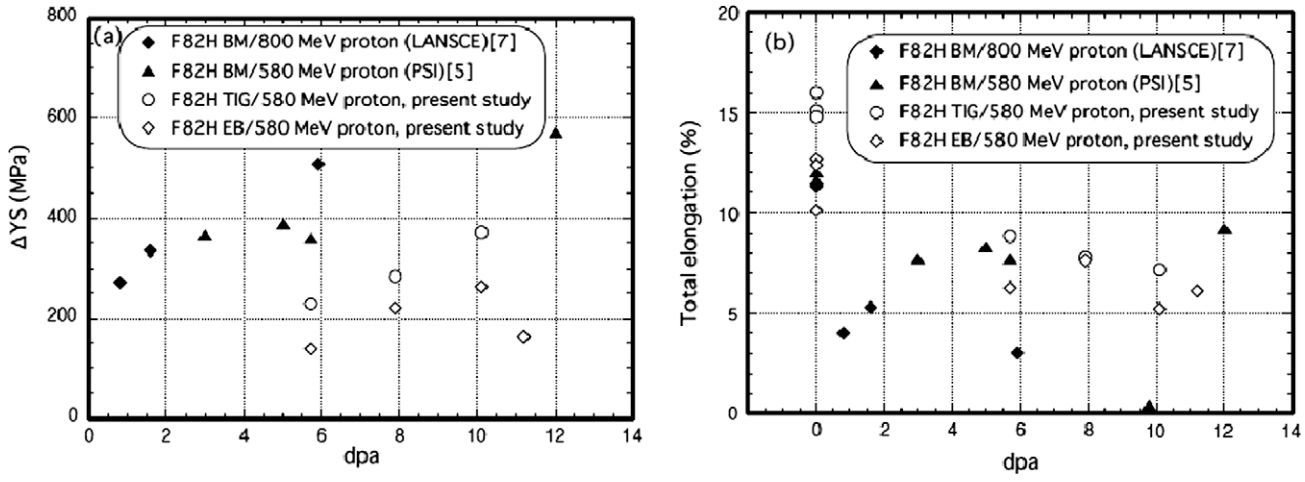

Fig. 12. The tensile properties of the proton-irradiated F82H welds and F82H BM. (a) shows the relationship between dpa and increase in YS. (b) shows the relationship between dpa and total elongation (TE). Test temperature was R.T.

5. Summary

Tensile properties on high-energy proton and spallation neutron irradiated F82H welds at 5.7–11.8 dpa were investigated. The results obtained from present study are summarized as follows:

(1) The results on tensile tests indicate that the irradiation hardening was observed up to 10.1 dpa at below 320 °C. At higher dose (11.8 dpa) and higher temperature (380 °C), irradiation hardening and degradation of ductility decreased.
(2) All tensile properties tested at RT and 250 °C were ductile.

Bend-fatigue properties on high-energy proton and spallation neutron irradiated F82H BM and F82H welds at 6.3–9.1 dpa were also investigated. The results obtained from present study are summarized as follows:

(1) Irradiation effects on the fatigue life vary with welds.
(2) The fatigue life of the F82H BM specimens irradiated by 6.3 dpa is almost the same with that of unirradiated specimens. The fatigue life of the specimens irradiated up to 9.1 dpa is slightly shorter from that of unirradiated specimens.
(3) F82H TIG specimens did not fracture during 10^7 cycles at maximum displacement. The fatigue life of F82H EB (15 mm) and EB (3.3 mm) seem to increase after the irradiation.
(4) The fracture surfaces of the specimens showed transgranular morphology. However an intergranular fracture surface is observed for both the unirradiated and irradiated F82H base metal specimens.

Acknowledgments

We greatly appreciate the helpful comments and supports given by the members of Hot Laboratory during this study.

References

[1] R.L. Klueh, K. Ehrlich, F. Abe, J. Nucl. Mater. 191–194 (1992) 116–124.
[2] A. Kohyama, A. Hishinuma, D.S. Gelles, R.L. Klueh, W. Dietz, K. Ehrlich, J. Nucl. Mater. 133–137 (1996) 138–147.
[3] K. Shiba, T. Sawai, Y. Kohno, A. Kohyama, Report of IEA Workshop on Reduced-Activation Ferritic/Martensitic Steels, JAERI-Conference 2001-07.
[4] P. Spatig, R. Schaublin, S. Gyger, M. Victoria, J. Nucl. Mater. 258–263 (1998) 1345–1349.
[5] Y. Dai, B. Long, Z.F. Tong, J. Nucl. Mater. 377 (2008) 115–121.
[6] Y. Dai, S.A. Maloy, G.S. Bauer, W.F. Sommer, J. Nucl. Mater. 283–287 (2000) 513–517.
[7] Y. Dai, X. Jia, S.A. Maloy, J. Nucl. Mater. 343 (2005) 241–246.
[8] Y. Dai, G.S. Bauer, J. Nucl. Mater. 296 (2001) 43–53.
[9] Y. Dai, Y. Foucher, M.R. James, B.M. Oliver, J. Nucl. Mater. 318 (2003) 167–175.
[10] A. Kohyama, K. Hamada, H. Matsui, J. Nucl. Mater. 179–181 (1991) 417–420.
[11] K. Kikuchi, S. Saito, Y. Nishino, K. Usami, in: Proceedings of Accelerator Applications in a Nuclear Renaissance (AccApp'03), San Diego, California, June, 2003, pp. 874–880.
[12] S. Saito, K. Kikuchi, Y. Onishi, Y. Nishino, J. Nucl. Mater. 307–311 (2002) 1609–1612.
[13] G.E. Dieter, Mechanical Metallurgy, vol. 289, McGraw-Hill, New York, 1986.
[14] H. Tanigawa, T. Hirose, M. Ando, S. Jitsukawa, Y. Katoh, A. Kohyama, J. Nucl. Mater. 307–311 (2002) 293–298.
[15] T. Hirose, H. Tanigawa, M. Ando, A. Kohyama, Y. Katoh, M. Narui, J. Nucl. Mater. 307–311 (2002) 304–307.
[16] Y. Miwa, S. Jitsukawa, M. Yonekawa, J. Nucl. Mater. 329–333 (2004) 1098–1102.
[17] P. Marmy, M. Vicrtoria, J. Nucl. Mater. 191–194 (1992) 862–867.
[18] R. Lindau, A. Moeslang, J. Nucl. Mater. 212–215 (1994) 599–603.
[19] M.L. Grossbeck, J.M. Vitek, K.C. Liu, J. Nucl. Mater. 141–143 (1986) 966–972.
[20] J. Bertsch, S. Meyer, A. Moeslang, J. Nucl. Mater. 283–287 (2000) 832–837.